International Journal of
INTELLIGENT SYSTEMS AND APPLICATIONS IN ENGINEERING
ISSN:2147-6799 www.ijisae.org Original Research Paper

Sensor Less BLDC Motor Drive Using a Multi-Sector Space Vector PWM Method Based on Adaptive Network-Based Fuzzy Inference System

[1]Ch. Vinay Kumar, [2]Dr. G. Madhusudhana Rao, [3]Dr. A. Raghu Ram

Submitted: 02/10/2023 **Revised:** 21/11/2023 **Accepted:** 01/12/2023

Abstract: This article describes the process of developing a MS-SVPWM controls BLDC motor rotational speed. This innovative control approach improves BLDC efficiency at a variety of speeds and loads. Construction of the prototype around a brushless DC motor with 400 W of output power, 30 V of voltage, and 3000 rpm of rotational speed. The drive's unregulated rectifier supplies the necessary DC current to the inverter. The desired drive control is an MS-SVPWM scheme with ANFIS control. By contrasting the operation of conventional space vector PWM& with that of a multi-sector SV-PWM system, ANFIS controllers can choose the best drive sector & detect mismatched pulses. This unique switching control mechanism not only improves the efficiency of the BLDC system but also reduces the switching losses experienced by the inverter. This MS-SVPWM effectively reduces undesired distortions like THD, torque, & DC voltage ripple. To check the feasibility of the proposed system, MATLAB Simulink simulations are run. System simulation and experimental findings for the RP2040-controlled MS-hardware SVPWM are presented.

Keywords: *BLDC drive, MS-SVPWM, ANFIS control, MATLAB Simulink, RP2040 controller.*

1. Introduction

There is less electrical noise, higher efficiency, and more usable torque at low speeds with a brushless DC motor compared to a conventional one. Because of this, it has found significant application in manufacturing. In DC/AC power conversion, Voltage Source Inverters (VSI) are employed for their versatility in power production across a wide variety of voltages and frequencies. An inverter's output can be changed with a high fundamental component and minimal harmonic distortion by employing a modulation approach [1]. Several scholarly descriptions of various PWM techniques can be found in the scholarly literature. Some research suggests that the performance of a drive can be greatly improved by employing a PWM technique [2]. This includes the reduction of EMI, torque ripple, induction motor noise, and voltage and current harmonics. The drawbacks were mitigated by several PWM strategies. Various pulse width modulation methods exist Sine-triangle PWM, SHE PWM, SVM, and Random PWM. Methods of pulse width modulation include.

Square Wave Modulation (SVM) is replacing Pulse Width Modulation (PWM) as the standard PWM for voltage supplied converter AC drives [3, 4]. In the context of SVM, it is feasible to use either a continuous or discontinuous modulation mode. When comparing discontinuous modulation to continuous modulation, switching losses are reduced by 33%.There are a wide range of space vector discontinuous modulation types to choose from. It all comes down to which sectors house the switches. Using the 0-, 30-, 60-, and 90-degree axes, you may rotate these regions through a whole 360 degrees [4]. Each sampling period returns a single '0' state. The constant switching and sampling rates suggest that these modulations belong to the deterministic pulse width modulation family. In all cycles, the order of the switches remains the same.

Methods utilising randomised phase-wise modulation (RPWM) switch between high- and low-frequency intervals at random. The fundamental flaw of the RPWM method is its inconsistent switching frequency. For the RPWM to work in a digital setting, an additional control algorithm is needed. Variable frequency drive is gaining support in industrial control. Controlling and estimating AC drives is harder than DC drives [5]. This intricacy grew as the drive's performance elevated. In scalar control, just the absolute value of the control variables is modified. However, flux and torque are regulated by other parameters, such as magnitude and frequency [6].

[1]*Assistant Professor Department of Electrical and Electronics Engineering Mahatma Gandhi Institute of Technology, Hyderabad*
vinayeee.mgit@gmail.com
[2]*Professor Department of Electrical Engineering O. P. Jindal University, Raigarh, Chhattisgarh, India*
gmrgurrala@gmail.com
[3]*Professor Department of Electrical and Electronics Engineering, JNTUHCEH, Hyderabad*
raghuram_a@yahoo.co.in

Therefore, vector control is more common in industrial settings than scalar control. Vector control employs the Field Oriented Control (FOC) strategy, which is inspired by the concept of the separately stimulated dc motor. The control algorithm for both flux and torque can be implemented with straightforward regulators using this method. Field-oriented control relies heavily on coordinate transformation. However, the correct rotor flux angle is required for transformations. Both direct and indirect FOC methods rely on the calculation of angles [7]. While mechanical speed is the key requirement of the Indirect FOC approach, a rotor flux estimator is the fundamental necessity of the Direct FOC method. In order for this technique to work, current controllers must be used. By shifting the relative position of the two flux vectors, DTC controls torque. Flux & torque control loops are essential to DTC systems. [8].

Although hysteresis control for digital-to-analog conversion (DTC) in an analogue arrangement is straightforward, DTC with a hysteresis controller employed in a DAP behaves somewhat differently from the analogue approach [9]. The quick torque and switching frequency of the DTC method, as well as the decreased harmonic loss, make it preferable to vector control. At low sampling frequencies, switching frequency and torque error are usually immune to hysteresis. band's influence. Increases in the hysteresis band cause a drop in switching frequency & an increase in torque error when using a fast sampling rate [10]. Thus, the conventional DTC method has flaws, such as erratic switching frequencies, substantial switching losses, and frequent sampling.

Closed-loop control [11] describes a system that maintains a constant rotational speed for a BLDC User-input brushless DC motor. Users can set the device to run the motor at 25%, 50%, or 75% of top speed. Digital signals of a particular type are referred to as "pulse width modulation" for convenience. One application of the pulse width modulator (PWM) is in sophisticated control circuits [12]. By using SV-PWM, A constant dc input produces a 15% more stable output voltage than pulse width modulation. Applied to multi-stage converters, this maximises dc link voltage use [13]. In comparison, it has lower THD and switching losses at a fixed switching frequency and Ma.

If you have a three-phase, three-leg inverter, you can set the line voltages to Vdc, zero, or some other value by using the inverter's six switches in various switching combinations. When using SVPWM, a rotating vector is employed to determine if and when the switch should be engaged [14]. Multiple PWM techniques have been developed and deployed to mitigate these shortcomings. In electronics, pulse width modulation (PWM) takes many forms [15]. Some examples include sin-triangle PWM, SHE PWM, SVM, and random-phase PWM. Space vector modulation (SVM) is a popular PWM for voltage fed converter drives due to its improved harmonic quality and increased linear range. This article explains how PWM pulses govern adaptive networks. ANFIS sensor-free closed-loop controls were tested on BLDC DTC systems [16]. Since electrical commutation every 60 degrees resolves the stator flux linkage amplitude, BLDC-DTC cannot affect it.

This system is called ANFIS—Adaptive Neural Fuzzy Inference System. The ANFIS toolbox function produces a FIS from an input/output data set by modifying the membership function values via back propagation or least squares. This may teach your fuzzy system anything about the data it represents. You can see a picture of the Takagi-ANFIS building down below. The rings show nodes that don't move, while the squares show nodes that do [17]. The ANFIS logic improves system performance in static & changing conditions. The fundamental network structure comprises all teachable ANFIS network paradigms. [18]. This controller doesn't try all of the rules when choosing what actions to take. Instead, it uses a subset of them. So, the suggested controller is better for real-time control than the standard ANFIS controller because it has more advantages, including a shorter execution time [19]. In an adaptive network, the general behaviour of inputs and outputs is set by node-connecting tuneable parameters.

This study shows how an ANFIS controller can control BLDC motor speed and torque using MS-SVPWM. Under penalty of higher switching losses [20], it also enables more accurate adjustment of the inverter's output voltage and enhanced drive performance. Organisation of the paper: an overview of the planned driving system, a description of the MS-SVPWM for the inverter, & finally, the results of the paper's simulations & hardware evaluations. This concludes the recommendations [21].

2. Proposed System

Adjustable speed drives (ASDs) can be used for a wide range of purposes. Because of its inexpensive price, low maintenance needs, and high output, induction motor drives (IMDs) are gaining in popularity. Unlike standard DC motors, BLDC ones sync their operations to the magnetic field's frequency. The magnetic fields in the rotor and stator spin at the same frequency [11]. Unlike conventional DC motors, which utilise brushes for commutation, BLDC motors can be controlled electronically. Over induction & Brushed DC motors, BLDC motors have several advantages. The motor's increased size and reduced weight make it a practical choice for these applications. Instead of "sliding" at low speeds like induction motors do, BLDC motors maintain

constant torque. Figure 1 depicts the three-phase, two-pole brushless DC motor (BLDC) used in this piece.

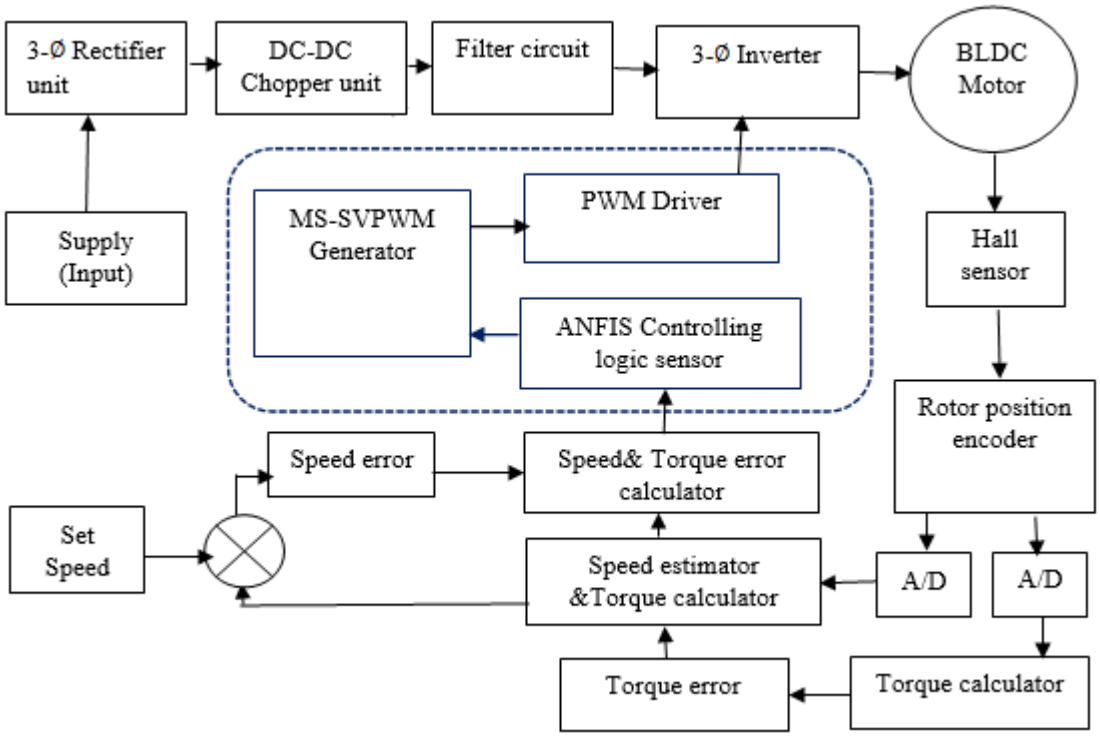

Fig 1. Proposed system BLDC Drive block diagram

With an angle of 120° conduction mode 3Ø BLDC motor, the signals of back EMF& phase current are shown below [22]. The analysis of BLDC motor may be observed in the circuit and equations below. With a BLDC drive, it is possible to formulate a mathematical model in by Solving algebraic-nonlinear differential equations [23]. The BLDC motor phase voltage formulae are below:

$$V_a = R_a I_a + L_a dI_a/dt + L_{ab} dI_b/dt + L_{ca} dI_c/dt + e_a \quad (1)$$

$$V_b = R_b I_b + L_b dI_b/dt + L_{ab} dI_a/dt + L_{bc} dI_c/dt + e_b \quad (2)$$

$$V_c = R_c I_c + L_c dI_c/dt + L_{ac} dI_c/dt + L_{bc} dI_b/dt + e_c \quad (3)$$

$$[V_a V_b V_c]. = [R000R000R][I_a I_b I_c] + [e_a e_b e_c][L - M000L - M000L - M]\, d/dt\,[I_a I_b I_c] \quad (4)$$

In this equation, V_a, V_b, V_c&I_a, I_b, I_c&e_a, e_b, e_c, are phase voltages, currents & back EMFs respectively, there are three constants in a circuit: the phase resistance, Self- and mutual inductances L and M. The magnetic torque can then be determined by using this formula.

$$T_e = (e_a I_a + e_b I_b + e_c I_c)/W_r) \quad (5)$$

Where $W_r$represents the rotor mechanical speed & motion is given as:

$$\frac{d}{dt}(W_r) = \frac{T_e - T_l - BW_r}{J} \quad (6)$$

For a centrifugal pump, the relationship between hydrodynamic load torque and rotational velocity looks like this: where B stands for J for driving inertia, T l for hydrodynamic load torque [24].

$$T = KW_r^2 \quad (7)$$

The relationship between K is the pump torque constant and for the motor with P poles, the electricity and mechanical speed. [25].

$$W_e = (P/2) \quad (8)$$

3. MS-SVPWM architecture based on ANFIS

PWM is often utilised to control the converter's power electronic changes. Converter circuit performance degrades in high voltage applications due to constant switching states. Constant switching between phases causes significant switching losses in the converter. In an effort to reduce the amount of energy wasted as heat by the power converter, numerous PWM techniques have been investigated. Power converters waste energy in the form of the developers created space vector pulse width modulation (SVPWM) to reduce switching losses. The SVPWM's symmetrical control means that the switching condition of each sector can be predicted.

Conventional SVPWM Technique: Regular space vector PWM creates the reference voltage vector by activating one of 8 different switching patterns for a fixed period of

time. See Figure 2 and consider the top half of the hexagon. A time-averaged amplitude space-vector (SV) at an angle =t from the d-axis requires the inverter to be at the sector border and zero. Maintain state (1,0,0) for T1, T2, and ZSVS for T0. In well-balanced SV modulation, V0 should worry about T0/2 and V7 about T7/2. According to Eq. (10), the inverter generates a time-averaged SV with amplitude Eq. (9). Carrier period Tz is defined as.

$$V_{ref} = V_1.T_1 + V_2.T_2 + V_0.T_0 \qquad (9)$$

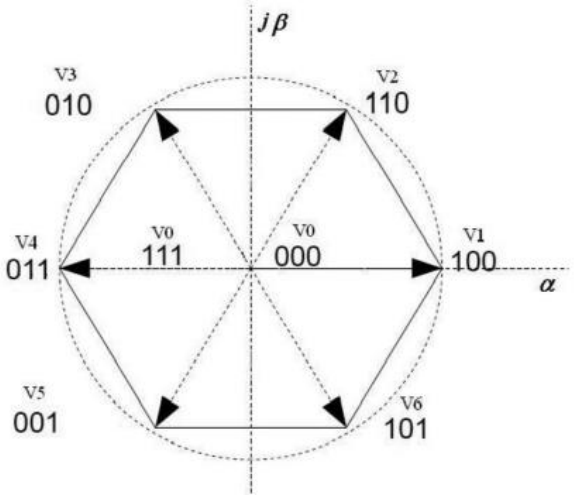

Fig 2. SVPWM basic switching vectors

$$T_z = T_1 + T_2 + T_0 \qquad (10)$$

To calculate & the angle (), the Clarke and Park transformation is employed. If you want to move from the a-b-c plane to the d-q plane, you can use A, B, C, D, Q: Clarke's transformation. According to Eqs. (11) and (12), the Park transformation transforms two axes into d and q. (12).

$$V_d = V_{an} - V_{bn}\cos 60 - V_{cn}\cos 60 = V_{an} - \frac{1}{2}V_{bn} - \frac{1}{2}V_{cn} \qquad (11)$$

$$V_q = 0 - V_{bn}\cos 30 - V_{cn}\cos 30 = V_{an} + \frac{\sqrt{3}}{2}V_{bn} - \frac{\sqrt{3}}{2}V_{cn} \qquad (12)$$

Time periods T1, T2, and T0 are determined using these steps;

Let's examine the first business niche. Vector states V0, V1, and V2 should be triggered at times T0, T1, and T2, accordingly. The entirety of time, denoted by Tz. Let's say 1 kilohertz (kHz) is the switching frequency we've decided upon. Tz=.00001 sec (1msec)

This case

$$\begin{bmatrix} K = \sqrt{3} \times T_z \times \frac{V_{ref}}{V_{dc}}; \\ T_1 = k \times \left(\sin(1.05 - (angle) + \left(\frac{(n-1)}{3}\right) \times 3.14)\right); \\ T_2 = k \times \left(\sin(angle) - \left(\frac{(n-1)}{3}\right) \times 3.14)\right); \end{bmatrix} \qquad (13)$$

$$T_0 = T_z - (T_1 + T_2);$$

$$Angle = \tan^{-1}\left(V_q / V_d\right)$$

And so, for the times that the switches in Sector 1 are on. To determine which vector combinations in time are most effective, it is sufficient to perform some relevant computations in each individual sector. The modulation index controls both the output voltage's frequency and its amplitude.

Propose Pseudo Code
MS-SVPWM Functional unit
Input:*Angle* *(α), voltage of d-q axis*
Output: Gate pulse

Steps:

1. Set the initial value of the reference voltage (V_{ref})
2. Determine the cause of the asymmetry in the voltage vector (V_{ni}, V_{nj} &V_{nk})
3. Information used to instruct the ANFIS controller
4. Determining the Times T 1, T 2, & T 0 All six VSI switch times (S 1 to S 6) are calculated.
5. A comparison between MSSVPWM and traditional SNPWM
6. Computation of a mismatched pulse
7. The VSI receives pulses from the MSSVPWM that have been error-corrected

End

Fig 3. MS-SVPWM Pseudo code

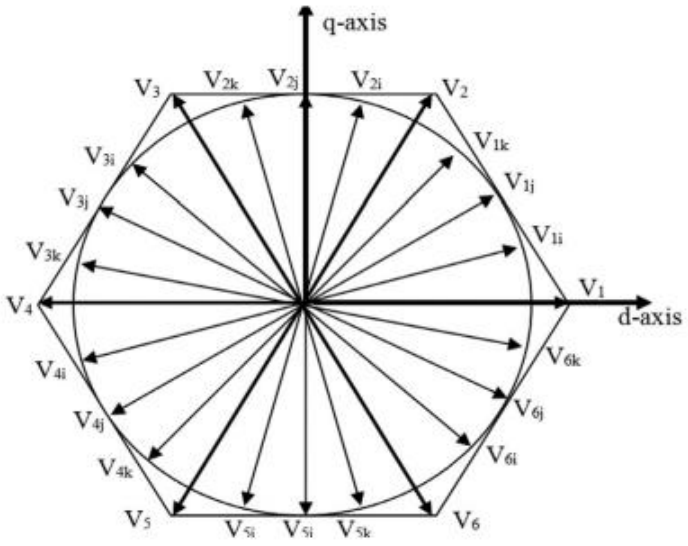

Fig 4. Representation of Hexagon MS-SVPWM.

The High-Speed Spatio-Velocity Pulse Width Modulation Scheme: In this research, researchers examine the in a VSI-based BLDC drive, Hybrid MS-SVPWM is used to dynamically alter the switching state. In Figure 3, we can see the transitions that occur throughout the MS-SVPWM implementation.

As a rule, 3-ØVSI's a total of eight distinct switching losses, with states 1-6 representing active switching and states 0 and 7 representing idle switching. Where =1,2,3,4,5,6, and the number of quarters is 4, the asymmetric voltage vector is denoted as,, & in MS-SVPWM. Figure 4 depicts the MS-SVPWM's sector count, which is 24. The MS-SVPWM 15° vector will be computed using the V1 and V2 are non-zero vectors, and V0 and V24 are zero vectors.

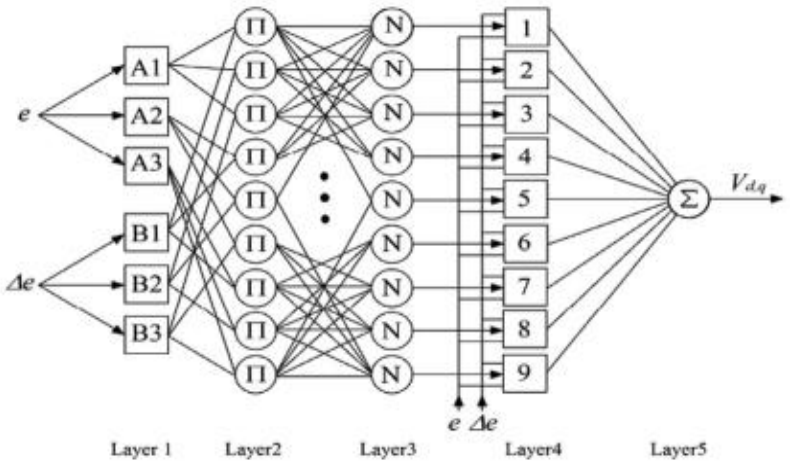

Fig 5. Structure of the ANFIS Suggested.

The conventional methods of control have been surpassed in effectiveness by both FLC and ANNs. Improved dynamic behaviour and faster convergence can be found in an ANFIS (Adaptive Neuro-Fuzzy Interface Systems) system as compared to FLC and ANN. Following the FLC rules in table 1, the ANFIS controller forms the basis for the MS-SVPWM implementation depicted in figure 5. The SV product at time t0 determines the inverter's dynamic switching behaviour. The initial voltage sector actively switching weights on the voltagevector are w1, w2, w3, w4, w5, and w6. Voltage vectors v0 and v7 are inactive partners for w0 and w7. Here, we employ the expected values of the hexagonal voltage magnitudes as weights.

Table 1. FLC's instructions

Outputs	**Δe**							
	$-NB$	**-NM**	**-NS**	**-Z**	**-PS**	**-PM**	**-PB**	
E	-NB	-NB	-NB	-NB	-NB	-NM	-NS	**-Z**
	-NM	-NB	-NB	-NB	-NM	-NS	-Z	**-PS**
	-NS	-NB	-NB	-NM	-NS	-Z	-PS	**-PM**
	-Z	-NB	-NM	-NS	-Z	-PS	-PM	**-PB**
	-PS	-NM	-NS	-Z	-PS	-PM	-PB	**-PB**
	-PM	-NS	-Z	-PS	-PM	-PB	-PB	**-PB**
	-PB	-Z	-PS	-PM	-PB	-PB	-PB	**-PB**

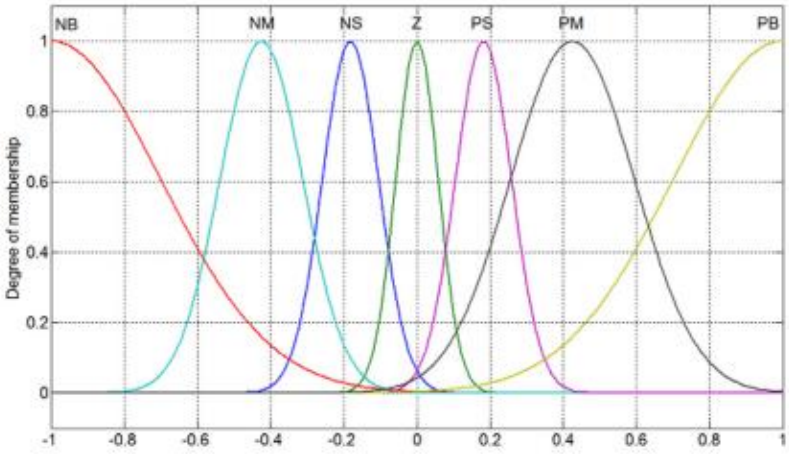

Fig 6. input/output functions before ANFIS training.

The vector and angle nearest the origin are given the most priority for generating MS-SVPWM based on their magnitude and divergence from the sector angle. The reference voltage vectors (14) will be calculated using equations (9), (10), and (11), respectively. We compare the performance of MS-continuous SVPWMs to that of their discontinuous counterparts over a wide range of loads, using both Simulink and experimental approaches.

The MS-SVPWM control based on ANFIS works very well as a VSI power supply for a BLDC motor drive. As can be observed in Figure6, the ANFIS controller design and training improves the system-wide stability.

ANFIS Controller: Setting up an ANFIS: The ANFIS controller & teaching it to fine-tune its initial fuzzy settings in order to perform the required control action in a variety of operational contexts is detailed.

Initialization: *Input load vector* $i^*_{d.q}$ & $i_{d.q}$ is to determine error (e) & change in error (Δe)

$$e = i^*_{d.q} - i_{d.q} \quad (16)$$

$$x = e(t) \quad (17)$$

$$\Delta e = e(k) - e(k-1) \quad (18)$$

Fig 7. Proposed system power circuit with RP2040 controller.

Figure 7 shows an RP2040 Controller used to govern a BLDC and MS-SVPWM. The three-phase BLDC voltage waveform is shown. Rapidly changing load conditions have skewed the system's output voltage, as shown in Figure 6.

$$y = \Delta e(t) \quad (19)$$

Select membership function from Ai=1 to 7

$$O_i^1 = \mu_{Ai}(x) = \frac{1}{1 + [[1/[x - C_i]/A_i]^{b_i}]} \quad (20)$$

$$O_{i+2}^1 = \mu_{Bi}(y) = \frac{1}{1 + [[1/\ [y - C_{i+2}]/A_{i+2}]^{b_{i+2}}]}$$

Forward pass: Here, we employ a rule inference layer. All interactions at this level are labelled, fixed nodes that multiply incoming signals and return the product. The activation of a fuzzy rule is proportional to each neuron's output.

$$O_i^2 = W_i + \mu_{Ai}(x)\mu_{Bi}(y) \quad (22)$$

Backward pass: This layer's focus is on achieving data normalisation. There are N nodes in this layer, and each one is a circle with the label "N" at its middle. The rule's efficacy is calculated as a percentage of all rules by the i-th node.

$$O_i^3 = \overline{W_i} = \frac{W_i}{\sum_i W_i} \quad (23)$$

$$O_i^4 = \overline{W_i} f_i = \overline{W_i}(p_i x + q_i y + r_i) \quad (24)$$

The properties of this node are denoted by pi, qi, and ri, whereas ANFIS stands for the average normalised firing intensity.

$$i = O_i^5 = \sum_i \overline{W_i} f_i \quad (21) \quad (25)$$

$$\frac{\delta E}{\delta O^5} = k_1 e + k_2 \Delta e \quad (26)$$

Training data: Multiplication of rate of change (e2) & input signals error (e) by the k1 & k2 coefficients.

$$\alpha_{k+1} = \alpha_k - \eta \frac{\delta E}{\delta k} \quad (27)$$

The proposed fuzzy structure requires value estimates for 21 premise and 14 consequence parameters. Here is the

process followed to compile the database used to teach the ANFIS the optimal I/O pattern:

i. The design process occurs in a wide range of configurations within the switching business, i.

ii. Second, repeat the first procedure using a variety of switching angles and loads.

iii. The resulting training pairs (Vd, Vq) are then utilised to design the fuzzy controller.

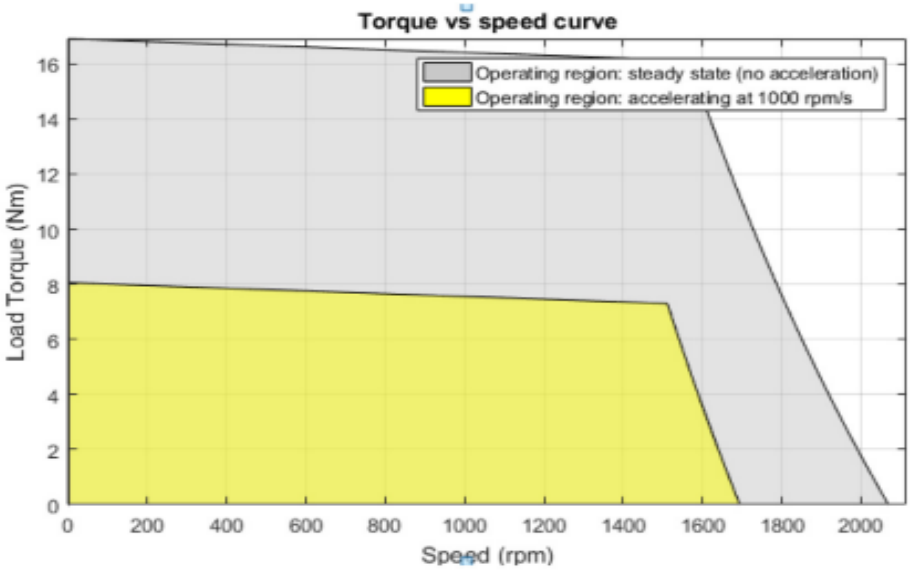

Fig 8. Curve between Torque & Speed.

Figure8 demonstrates that the speed response using the proposed speed controller is practically the same with and without the load disturbance. As a result, the proposed controller ensures the steadiness of the system.

4. Results and Discussions

A three-phase, three-direct current (BLDC) motor rated at 400 watts was used for this task. Several situations are simulated, such as starting up, running smoothly, experiencing a sudden change in load, and switching the direction the motor is spinning in. The torque, flux, and ripple in Figure 9(a)-(f) are also indicative of a more steady state-like condition. In this study, we propose employing Discontinuous MSSVPWM methods to reduce steady-state ripple. Hybrid vector control technique proposed greatly reduces the steady-state torque ripple, flux, and current compared to conventional methods.

Table 2. Parameters of BLDC motor drive.

Parameter	**Quantity**	**Parameter**	**Quantity**
Friction	0.005N m-s	I/P phase-phase voltage (AC)	@220 V
L (Inductance)	$08.50e^{-3}$ H	Diode ON state resistance	$01.0e^{-3}$
Torque constant	104 N-M	IGBT's forward voltage	00.8 V
Flux linkage	0.175	Breaking chopper resistance	8 ohms
V constant (V peak)	147.00 V	Inverter's IGBT's ON state resistance	$01e^{-3}$ ohms
Equivalent circuit resistance	0.2 ohm	Snubber capacitance	$20e^{-9}$
Snubber resistance	10 e^{3} ohm	Power	3 HP
Inertia	0.089kg*sq. m	Chopper frequency	4000Hz
Back EMF flat area	120	Forward voltage	1.3V
Poles pair	4	Speed	1650 rpm

Simulation results: MATLAB Research into Simulation of BLDC motor drive using Simulink. The simulation inquiry parameters are in Table2. Parameter under load fluctuations when there is uncertainty further improves speed performance.

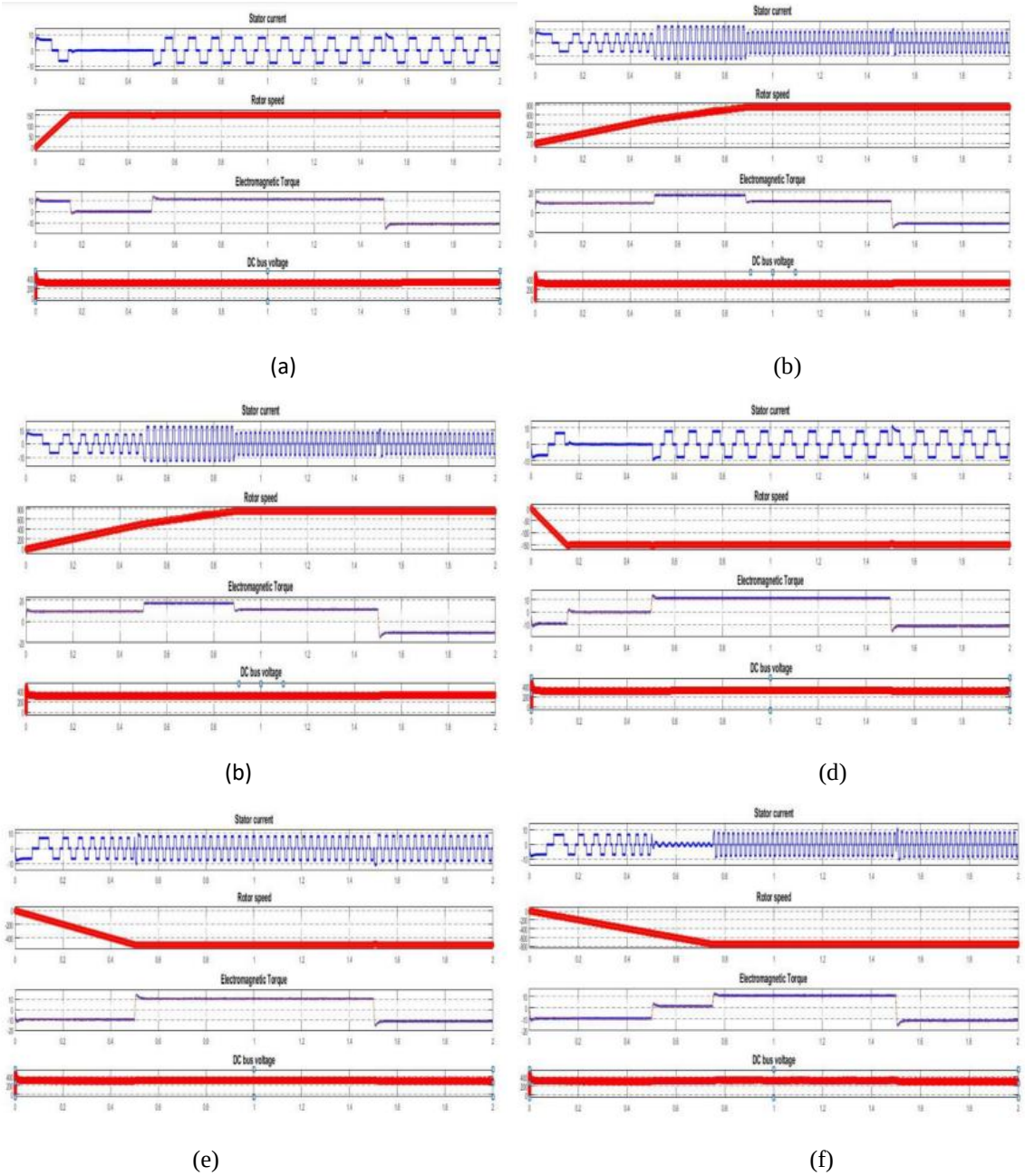

Fig 9. MS-SVPWM current, torque, speed, and DC voltage for the stator of a clockwise-rotating BLDC drive direction. Rated load of (a) 20% (b) 50% (c) 100% and with anticlockwise direction (d) 20% (e) 50% (f) 100%.

Experimental results: Parameters describing the BLDC drive's presentation are shown in Figure 9. The authors utilised an RP2040 Controller to manage a BLDC and MS-SVPWM. The research revealed BLDC generated a three-phase voltage waveform like this. Rapid load changes distort the system's output voltage. Regulation of transient distortion in a VSI's output voltage is made possible by implementing MS-SVPWM in a digital signal processor controller.

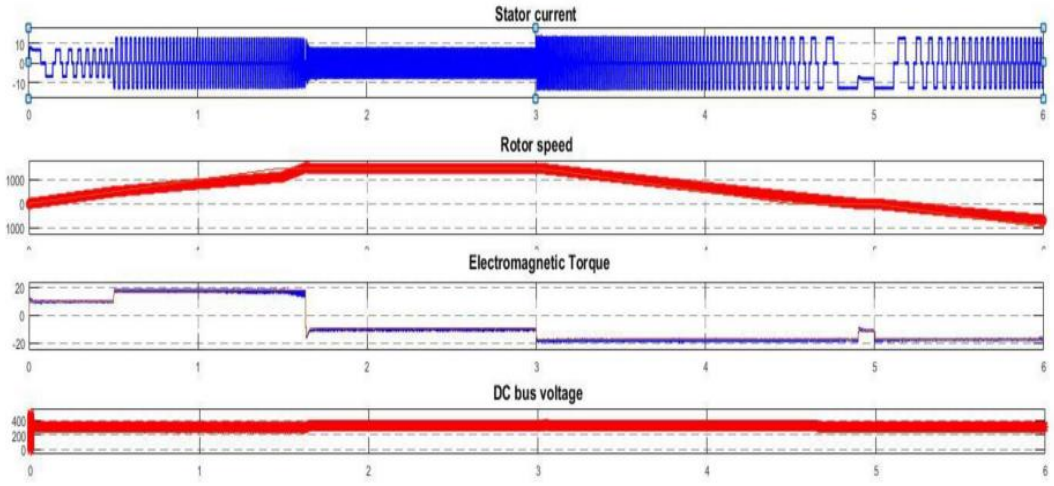

Fig 10. BLDC drive's output waveforms with clockwise & anticlockwise direction.

As can be seen in Figure 10, The BLDC motor drive delivers electromagnetic torque identical to the TL and has little torque ripple. While changing directions and loads. Use FLUKE power quality analyzer and Power log software, you can determine the number of harmonics present in the VSI's three-phase output current. Figure 11(a) and Figure 11(b) depict the results of measurements taken of THD(b) is the Total Harmonic Distortion measured at the load current.

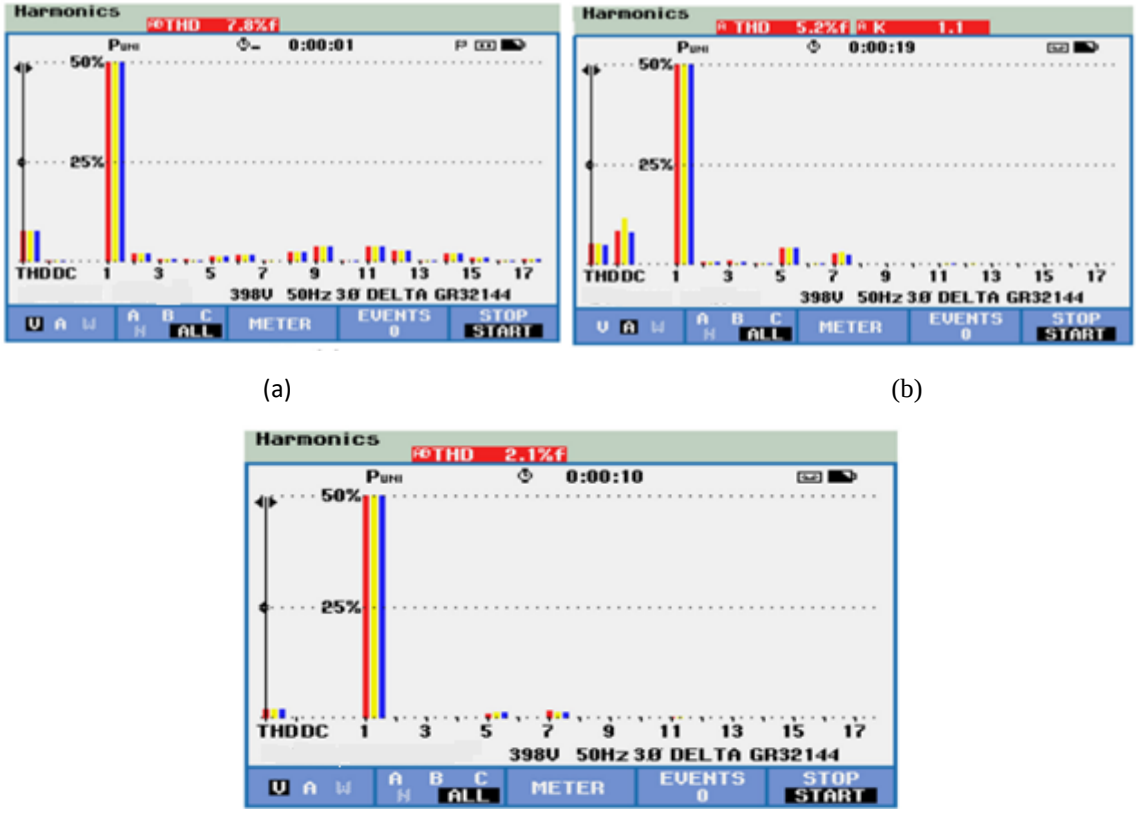

(a) (b)

(c)

Fig 11. MS-SVPWM's THD% of rated load (a) 20% (b) 50% (c) 100%.

Figure12 shows how the output reference voltage is modified by the MS-SVPWM controller in response to load changes and speed reversals. As can be seen in figures 13 and 14, the proposed ANFIS based MSSVPWM system effectively decreased distortion of current& widened the current rebuilding range of 3-phase Inverter, with the latter being a function of the size of the DC-link voltage.

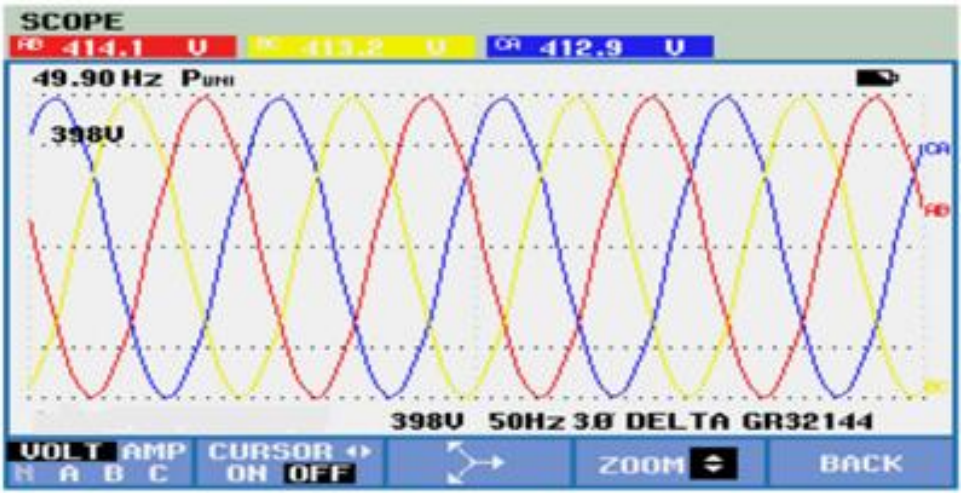

Fig 12. MS-SVPWM's output waveforms with 100% of rated load.

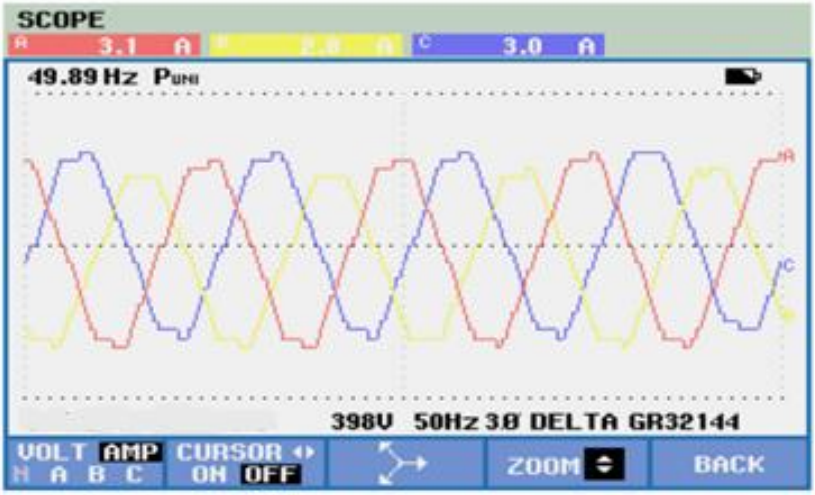

Fig 13. BLDC drive's current waveforms.

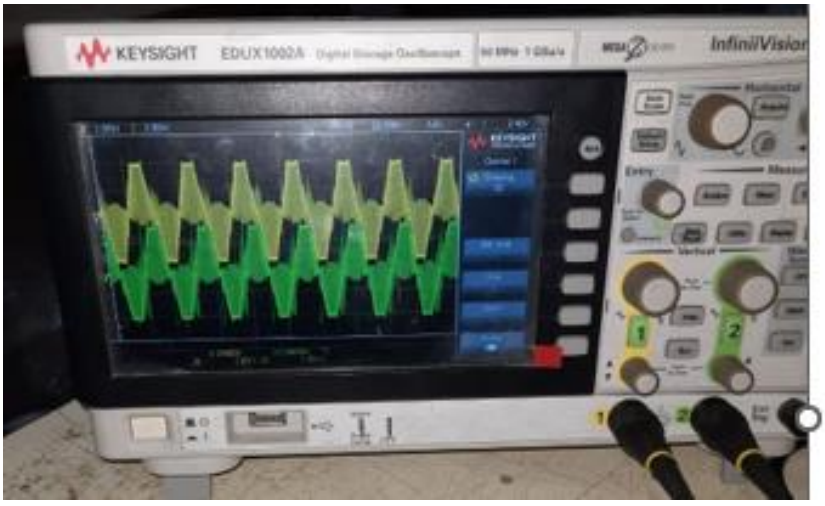

Fig 14. proposed system output waveforms.

The suggested MS-SVPWM, which utilises ANFIS control, has a superior time response in speed settling, with a delay of around 10 seconds, observed in both the positive and negative speed segments of the speed curve. The system successfully attains a speed of 994 rpm, which is in close proximity to the desired target speed of 1000 rpm. The Total Harmonic Distortion (THD) has greater significance for average operating speeds, wherein its magnitude reaches a minimum threshold of 2.1%. The utilisation of Modified Sine Space Vector Pulse Width Modulation (MS-SVPWM) results in a reduction of approximately 5% in ripple within its rated torque when compared to standard Pulse Width Modulation (PWM) controllers.

5. Conclusion

Standard BLDCs are simple to use and respond quickly. Still, when it is in a steady state, torque, flux, and current all show a wave. This study shows a new mixed asymmetrical SVPWM method for driving BLDC motors. In this combination method, the best voltage vectors to use are chosen with the help of an ANFIS control system. A sample hardware version using an RP2040 controller has been made that can drive a 400 WBLDC motor. With the help of ANFIS, Controller sector selection is complete. Optimisation of switching losses, torque ripples, stator current fluctuations, and Driven system settle time is possible. Modelling shows that the suggested strategy reduces torque steady-state ripples, flux, and current. Comparisons show that ANFIS-based BLDC has a lower time to steady-state than fuzzy-based. The recommended strategy could reduce inverter switching losses. Speed performance is improved via a hybrid vector controller. Parameter errors and load force changes are handled. Simulations and hardware experiments show that the proposed approach works effectively at many speeds.

References

[1] Malla, S. G., Malla, P., Malla, J. M. R., Singla, R., Choudekar, P., Koilada, R., & Sahu, M. K. (2022). Whale optimization algorithm for PV based water pumping system driven by BLDC motor using sliding mode controller. IEEE Journal of Emerging and Selected Topics in Power Electronics, 10(4), 4832-4844.

[2] Lins, A. W., & Krishnakumar, R. (2022). Tuning of PID controller for a PV-fed BLDC motor using PSO and TLBO algorithm. Applied Nanoscience, 1-24.

[3] Kumar, N. S., Chandrasekaran, G., Thangavel, J., Priyadarshi, N., Bhaskar, M. S., Hussien, M. G., ... & Ali, M. M. (2022). A Novel Design Methodology and Numerical Simulation of BLDC Motor for Power Loss Reduction. Applied Sciences, 12(20), 10596.

[4] Teoh, J. Y., & Yahya, J. A. F. (2022). Switching Scheme for Regenerative Braking Mode for BLDC Motor Driver. Evolution in Electrical and Electronic Engineering, 3(2), 801-807.

[5] Chan, J. W. (2022). Sliding Mode Control of Brushless DC Motor Speed Control. Malaysian Journal of Science and Advanced Technology, 188-193.

[6] Kommula, B. N., & Kota, V. R. (2022). An effective sustainable control of brushless DC motor using firefly algorithm–artificial neural network based FOPID controller. Sustainable Energy Technologies and Assessments, 52, 102097.

[7] Ch.Vinay Kumar, A.Raghu Ram & G.Madhusudhana Rao (2022, December). Optimized Evaluation of Brushless DC Motor Drive System using Adaptive Neuro-Fuzzy, PSO & Inference of genetic Algorithm. Journal of Northeastern University, (pp 1348-1355)

[8] Hameed, H. S. (2018, January). Brushless DC motor controller design using MATLAB applications. In 2018 1st International Scientific Conference of Engineering Sciences-3rd Scientific Conference of Engineering Science (ISCES) (pp. 44-49). IEEE.

[9] Damodharan, P., Sandeep, R., & Vasudevan, K. (2008). Simple position sensorless starting method for brushless DC motor. IET Electric Power Applications, 2(1), 49-55.

[10] Veni, K. K., Kumar, N. S., &Gnanavadivel, J. (2017, September). Low-cost fuzzy logic-based speed control of BLDC motor drives. In 2017 International Conference on Advances in Electrical Technology for Green Energy (ICAETGT) (pp. 7-12). IEEE.

[11] Sreeram, K. (2018, March). Design of fuzzy logic controller for speed control of sensorless BLDC motor drive. In 2018 international conference on control, power, communication and computing technologies (ICCPCCT) (pp. 18-24). IEEE.

[12] Satar, M. N. A., & Ishak, D. (2011, May). Application of Proteus VSM in modelling brushless DC motor drives. In 2011 4th International Conference on Mechatronics (ICOM) (pp. 1-7). IEEE.

[13] Ch.Vinay Kumar, G.Madhusudhana rao, A.Raghu Ram, & Y.Prasanna Kumar (2022, July). Designing of Neuro-Fuzzy Controllers for Brushless DC Motor Drives Operating with Multiswitch Three-Phase Topology. Hindawi, Journal of Electrical and Computer Engineering(pp.1-12)

[14] Vinayaka, K. U., & Priya, S. (2016, April). Analysis of BLDC motor performance using space vector pulse width modulation. In 2016 International Conference on Computation of Power, Energy Information and Commuincation (ICCPEIC) (pp. 549-552). IEEE.

[15] Viswanathan, V., &Jeevananthan, S. (2011). A Novel Current Controlled Space Vector Modulation based Control Scheme for Reducing Torque Ripple in Brushless DC Drives. International Journal of Computer Applications, 28(2), 25-31.

[16] Gujjar, M. N., & Kumar, P. (2017, May). Comparative analysis of field-oriented control of BLDC motor using SPWM and SVPWM techniques. In 2017 2nd IEEE International Conference on Recent Trends in Electronics,

Information & Communication Technology (RTEICT) (pp. 924-929). IEEE.

[17] Singh, J., & Singh, M. (2016). Comparison and analysis of different techniques for speed control of brushless DC motor using matlabsimulink. International Journal of Engineering Trends and Technology-IJETT, 38(7), 373-379.

[18] Ch.Vinay Kumar, A.Raghu Ram & G.Madhusudhana Rao (2022, December). Design and Development of Remora Optimization based Controller for Speed Management in Three-Phase Brushless DC Motor. NeuroQuantology Journal, (pp 1901-1923)

[19] Santra, S. B., Chatterjee, A., Chatterjee, D., Padmanaban, S., & Bhattacharya, K. (2022). High efficiency operation of brushless dc motor drive using optimized harmonic minimization-based switching technique. IEEE Transactions on Industry Applications, 58(2), 2122-2133.

[20] Mukherjee, A., Ray, S., & Das, A. (2014). Development of microcontroller-based speed control scheme of BLDC motor using proteus VSM software. International Journal of Electronics and Electrical Engineering, 2(1), 1-7.

[21] John Prabu, M., Poongodi, P., & Premkumar, K. (2016). Fuzzy supervised online coactive neuro-fuzzy inference system-based rotor position control of brushless DC motor. IET Power Electronics, 9(11), 2229-2239.

[22] Aspalli, M. S., Munshi, F. M., &Medegar, S. L. (2015, August). Speed control of BLDC motor with four switch three phase inverter using digital signal controller. In 2015 International Conference on Power and Advanced Control Engineering (ICPACE) (pp. 371-376). IEEE.

[23] Chougale, R. G., &Lakade, C. R. (2017, September). Regenerative braking system of electric vehicle driven by brushless DC motor using fuzzy logic. In 2017 IEEE International Conference on Power, Control, Signals and Instrumentation Engineering (ICPCSI) (pp. 2167-2171). IEEE.

[24] Karpagaraj, A., Edberk, J. A. S., Kannan, T. D. B., Rajendran, D. K., & Ramesh, T. (2022). Effect of GTAW process parameters on joining stainless steel 316L. *PROCEEDINGS OF THE INTERNATIONAL CONFERENCE ON RECENT ADVANCES IN MANUFACTURING ENGINEERING RESEARCH 2021: ICRAMER 2021*. Presented at the PROCEEDINGS OF THE INTERNATIONAL CONFERENCE ON RECENT ADVANCES IN MANUFACTURING ENGINEERING RESEARCH 2021: ICRAMER 2021, Chennai, India. doi:10.1063/5.0095789

[25] Vijetha, T., & Krishna, D. R. (2022, December 12). Dual band notch antenna for ultra wide band applications. *2022 IEEE Microwaves, Antennas, and Propagation Conference (MAPCON)*. Presented at the 2022 IEEE Microwaves, Antennas, and Propagation Conference (MAPCON), Bangalore, India. doi:10.1109/mapcon56011.2022.10046691

[26] Agarwal, S. K., Ramesh, S. M., Kumar, A. A., Yadav, S., Nagalakshmi, M., & Singh, P. (2022, December 23). A microservices-based IoT applications in Edge computing environments. *2022 2nd International Conference on Innovative Sustainable Computational Technologies (CISCT)*. Presented at the 2022 2nd International Conference on Innovative Sustainable Computational Technologies (CISCT), Dehradun, India. doi:10.1109/cisct55310.2022.10046492

[27] Haritha, I. V. S. L., Harshini, M., Patil, S., & Philip, J. (2022, December 1). Real Time Object Detection using YOLO Algorithm. *2022 6th International Conference on Electronics, Communication and Aerospace Technology*. Presented at the 2022 6th International Conference on Electronics, Communication and Aerospace Technology (ICECA), Coimbatore, India. doi:10.1109/iceca55336.2022.10009184

[28] Haritha, I. V. S. L., Harshini, M., Patil, S., & Philip, J. (2022, December 1). Real Time Object Detection using YOLO Algorithm. *2022 6th International Conference on Electronics, Communication and Aerospace Technology*. Presented at the 2022 6th International Conference on Electronics, Communication and Aerospace Technology (ICECA), Coimbatore, India. doi:10.1109/iceca55336.2022.10009184

[29] Nagaraju Thatha, V., Srinivas Rao, A., Rajasekhar Reddy, N. V., & Silparaj, M. (2022, October 3). Application of Hyper parameter Optimization Algorithms using Big Data. *2022 13th International Conference on Computing Communication and Networking Technologies (ICCCNT)*. Presented at the 2022 13th International Conference on Computing Communication and Networking Technologies (ICCCNT), Kharagpur, India. doi:10.1109/icccnt54827.2022.9984469

[30] Srinivas Rao, K., Divakara Rao, D. V., Patel, I., Saikumar, K., & Vijendra Babu, D. (2023). Automatic Prediction and Identification of Smart Women Safety Wearable Device Using Dc-RFO-IoT. Journal of Information Technology Management, 15(Special Issue), 34-51.